

# Nanotube Surface Functionalization Effects in Blended Multiwalled Carbon Nanotube/PVDF Composites

G. O'Bryan, E. L. Yang, T. Zifer, K. Wally, J. L. Skinner, A. L. Vance

Materials Chemistry Department, Sandia National Laboratories, Livermore, CA 94551

Received 20 April 2010; accepted 16 August 2010

DOI 10.1002/app.33264

Published online 24 November 2010 in Wiley Online Library (wileyonlinelibrary.com).

**ABSTRACT:** A mixed fill system of multiwalled carbon nanotubes (MWCNT) and hydroxylated MWCNT (HO-MWCNT) in a poly(vinylidene fluoride) (PVDF) matrix was investigated to improve nanotube dispersion and enhance electrical percolation for the bulk nanocomposites. Nonfunctionalized MWCNT were blended at various concentrations into dimethylformamide solutions containing PVDF with 0, 5, or 10 wt % HO-MWCNT. Composite samples prepared from these solutions were examined by four-point probe resistivity measurements. The percolation threshold decreased from 0.49 wt % MWCNT in binary MWCNT/PVDF composites to 0.25

wt % for ternary composites containing MWCNT/HO-MWCNT/PVDF, with either 5 or 10 wt % HO-MWCNT. In the case of the ternary composite with 10 wt % HO-MWCNT, the lowest fill percent of MWCNT (0.25 wt %) measured a conductivity that was three orders of magnitude higher than the binary MWCNT/PVDF composite containing twice the concentration of MWCNT (0.5 wt %). © 2010 Wiley Periodicals, Inc. *J Appl Polym Sci* 120: 1379–1384, 2011

**Key words:** nanocomposites; carbon nanotubes; dispersions; mixing

## INTRODUCTION

Carbon nanotube (CNT)-filled polymer nanocomposites are promising materials for a variety of applications,<sup>1</sup> with enhanced mechanical, thermal, and electronic properties imparted to the polymer matrix by mixing even minute amounts (<0.1 wt %) of CNTs. Of particular interest is the formation of CNT networks in a polymer film to create electrically conductive pathways. However, an efficient method for imparting the high electrical conductivity of individual CNTs to a composite material remains elusive. For a network of CNTs to form an electrically conductive path requires a minimum overlap of tubes, which is otherwise known as the percolation threshold. Van der Waals interactions between CNTs lead to aggregation and bundling into large clusters, which are a fundamental challenge to achieve maximum dispersion and conductivity for a given amount of CNTs. To compensate for this aggregation and achieve a conductive pathway through a filled polymer matrix, the fraction of CNTs is generally increased beyond the minimum fill required for

a theoretical percolation network. Therefore, a number of researchers have attempted to increase the dispersion of CNTs in various matrix materials through pretreatment functionalization methods and mixing procedures to obtain enhanced properties at lower fill percentages.<sup>2</sup> Generally, the increased dispersion from functionalization of CNT outer walls comes at the expense of carbon-carbon bond cleavage and reduction in the  $\pi$ -bonding network, which leads to a loss of electrical conductivity.<sup>3</sup> Another popular CNT dispersion enhancement strategy is to utilize small molecule and oligomeric additives that have high affinity for the CNT surface and can wrap around tubes to reduce aggregation via noncovalent functionalization.<sup>4</sup> This strategy has proven highly useful at maintaining the desired charge transport properties of CNTs while enhancing dispersion to form percolated networks at lower fill percentages.

In the process of exploring CNT-filled polymers for electromagnetic coating technologies, we developed a binary mixed fill system using hydroxy functionalized multiwalled carbon nanotubes (HO-MWCNT) with unfunctionalized MWCNT in a poly(vinylidene fluoride) (PVDF) matrix. PVDF was chosen as the matrix material in this study due to the excellent coating properties, viz. high durability, solvent resistance, low creep, etc., while maintaining solution processability for casting thin films of composite materials. The mixed fill system was chosen to explore the interaction of highly dispersible HO-MWCNT on the dispersion of commercial MWCNT.

Correspondence to: G. O'Bryan (gobryan@sandia.gov).

Contract grant sponsor: Laboratory Directed Research and Development Program at Sandia National Laboratories (for the United States Department of Energy); contract grant number: DE-AC04-94-AL85000.

Sun et al.<sup>5</sup> recently reported on a model with experimental support to understand the interaction of mixed fill systems composed of carbon black or graphite with MWCNT. They found that a lower percolation threshold can be reached in a mixed fill system based on the excluded volume theory. The network formation is a cooperative support system where the long aspect ratio of MWCNTs connects aggregates of carbon black to form conductive pathways. Recently, Spitalksy et al.<sup>6</sup> have demonstrated the effects of various oxidative treatments on MWCNTs in epoxy composites. They found that stronger oxidative treatments decrease electrical conductivity due to damage to the MWCNT outer wall and disruption of the  $\pi$ -bonding network. In contrast, weak oxidative treatments lead to improvement in the flexural modulus and electrical conductivity of epoxy composites. Similarly, Jung et al.<sup>7</sup> have recently reported that improved dispersion occurs as a result of vacuum ultraviolet oxidative treatment of MWCNT provides enhanced thermal, electrical, and mechanical properties. They demonstrate that at higher functionalization boundaries a degradation in the nanotube performance is observed and partial oxidation presents the optimal enhancement of desirable material properties. Herein, the present report discusses a phenomenon where blending oxidized MWCNTs with untreated MWCNTs in a PVDF nanocomposite leads to enhanced electrical characteristics. The enhanced electrical properties are observed at lower fills of untreated MWCNT compared with a nonblended (strictly untreated MWCNT/PVDF composites) system.

## EXPERIMENTAL

### Materials and sample preparation

MWCNTs were purchased in powder form from Cheap Tubes, with a purity of >95%, a tube diameter range of 8–15 nm, and length of 10–50  $\mu\text{m}$ . The MWCNTs were purified by washing with concentrated hydrochloric acid followed by a rinse with deionized water and a subsequent drying step in an oven at 120°C for 18 h. HO-MWCNTs purchased from Sun Innovations (Sun<sub>nano</sub>) in powder form, with a purity of 95%, a tube diameter range of 30–50 nm, and length of 10–20  $\mu\text{m}$  were used as received. PVDF in pellet form, purchased from Sigma-Aldrich, had a weight average molar mass ( $M_w$ ) of 180 kDa and a number average molar mass ( $M_n$ ) of 71 kDa.

Solutions of PVDF in dimethylformamide (DMF) were prepared by heating preweighed pellets in a water bath at 80°C with mechanical stirring until the pellets completely dissolved. Nanotubes were

weighed on an analytical balance, placed directly in PVDF solution, and vortexed to premix the solution. The solution was chilled in an ice bath, and an ultrasonication probe tip was placed in the solution for sonication at a power output of 14 W for 10 min. Sonicated solutions were drop casted on glass plates and dried in a vacuum oven at 70°C until the solvent was completely removed and the composite surface was no longer glossy (about 10–15 min). After cooling to room temperature, samples for resistivity measurements were cut on the glass plate into 4-cm-diameter circles and then peeled off.

### Instrumentation

Ultrasonication was performed with a Sonics 750 W Vibra Cell ultrasonication processor with a  $\frac{1}{4}$  in. microtip attachment operating at 35% amplitude. Microscopy was performed on a Hitachi scanning electron microscope S-4500 with an accelerating voltage of 15 kV. Electrical resistivity measurements were performed with a Jandel RM3-AR I-V source-meter using a Guardian SRM-232-10 four-point sheet resistance probe with a 62.5-mil spacing. A 100- $\Omega$  resistor supplied by the manufacturer was used to calibrate the instrument. Fourier transform infrared (FTIR) spectroscopy was performed on a Varian Scimitar Series 800; solutions of composite material were cast onto transparent KBr plates for measurement. Raman spectroscopy was performed using the 532-nm line of a Nd:YAG laser as the excitation source. The total power incident on the substrate surface was  $\sim 2$  mW and the laser spot size was  $\sim 650$  nm in diameter. Spectra were collected for an interval of 60 s. Differential scanning calorimetry (DSC) was performed on a Mettler Toledo DSC822<sup>e</sup> heating from room temperature to 200 °C at a rate of 2° per min in a 40- $\mu\text{L}$  aluminum pan with a blank pan for reference.

## RESULTS AND DISCUSSION

### Dispersion of MWCNT in a PVDF matrix

CNTs are generally blended into a polymer matrix via melt, extrusion, or solution mixing. As we are concerned with thin film applications of polymer nanocomposites, we chose a solution-based process for easy application either via spin, dip or drop casting of solutions. To prepare samples, PVDF was first dissolved into a DMF solution, typically in 8–10 wt % concentrations. The original solvent choice for this solution process was *N*-methylpyrrolidone, which creates excellent dispersions of CNT/polymer composites but is much more difficult to remove by evaporation after casting. MWCNTs were then blended into polymer solutions via ultrasonication

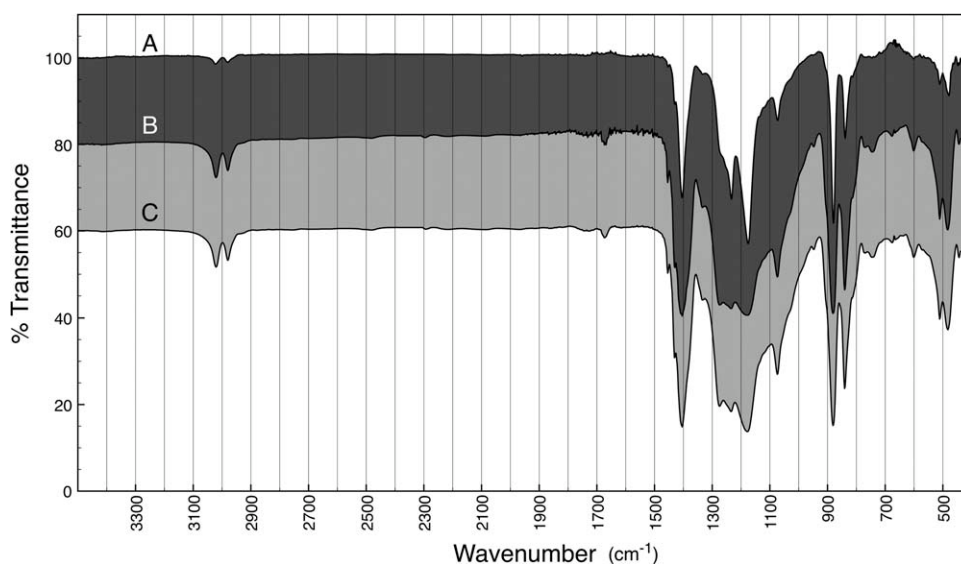


**Figure 1** Overlay of FTIR spectra of (A) PVDF, (B) PVDF with 1 wt % MWCNT, and (C) PVDF with 1 wt % HO-MWCNT.

to disperse tubes into the media. Sonication times were kept brief ( $\sim 10$  min) to minimize tube degradation.<sup>8</sup> Solutions prepared in this manner were stable for about 3 months, after this time, a noticeable clear solvent layer could be observed on top of settled composite material. Solutions of 1 wt % MWCNTs and 1 wt % HO-MWCNTs in PVDF were examined by FTIR spectroscopy to determine interaction effects with the matrix. Undoped PVDF, Figure 1(A), has characteristic peaks at 445, 512, 840, and 1175  $\text{cm}^{-1}$  corresponding to the  $\beta$  crystalline phase of PVDF.<sup>9</sup> No peaks were detected that correspond to the  $\alpha$  crystalline PVDF phase, consistent with reports of PVDF crystal phases evolving from DMF solutions.<sup>10</sup> PVDF films doped with 1 wt % MWCNT and 1 wt % HO-MWCNT produced virtually identical spectra. Enhancement of the  $\beta$  crystalline phase of PVDF was observed in both nanocomposite samples with peaks at 512 and 840  $\text{cm}^{-1}$  increasing most dramatically. Interestingly, in the case of PVDF with 1 wt % HO-MWCNT [cf. Fig. 1(B)], no broad signal was detected between 3200 and 3600  $\text{cm}^{-1}$ , a typical absorption for most hydrogen bonded hydroxyl groups.<sup>11</sup> Casting HO-MWCNT without PVDF and examining the material by FTIR also did not yield the expected H—O signal. Even still, the dispersion of HO-MWCNT in DMF and PVDF solutions remained much higher than unfunctionalized MWCNT.

DSC was performed on composites of PVDF to determine crystallinity and observe thermal behavior in polymer–MWCNT composites. Table I contains results from the thermal analysis for a pure PVDF film and two PVDF nanocomposites, one nonfunctionalized and the second functionalized. No

decrease in the polymer melt temperature ( $T_m$ ) was observed in either nanocomposite, but a change in the polymer crystallinity reveals an association difference between the functionalized and nonfunctionalized nanotubes and the matrix material. The decreased crystallinity of the nonfunctionalized nanotube PVDF composite (Table I, entry 2) is most likely the result of increased crystallite nucleation, consistent with the decrease in crystallinity observed in other PVDF CNT composite systems.<sup>12</sup> However, the HO-MWCNT PVDF nanocomposite (Table I, entry 3) has virtually the same crystallinity as the pure PVDF material indicating a favorable CNT polymer interaction and therefore a decrease in the number of nucleation sites.

Solutions of 1 wt % MWCNTs and 1 wt % HO-MWCNTs in PVDF were examined by Raman spectroscopy for further analysis. Two peaks were observed at 1350  $\text{cm}^{-1}$  and 1590  $\text{cm}^{-1}$ . The first peak, at 1350  $\text{cm}^{-1}$ , corresponds to the disorder mode or D band and the second peak, at 1590  $\text{cm}^{-1}$ , corresponds to the graphitic tangential mode or G band. In SWCNTs, an increase in the D to G band intensity is usually used to signify functionalization of the tubes. The change is attributed to defect sites forming during the transformation of carbon atoms

**TABLE I**  
Differential Scanning Calorimetry Results for PVDF Nanocomposites

Entry	Composite sample	$T_m$ ( $^{\circ}\text{C}$ )	$\Delta H$ ( $\text{Jg}^{-1}$ )	$X_c$ (%)
1	PVDF	173.6	32.2	31
2	2 wt % MWCNT	173.6	29.0	28
3	2 wt % HO-MWCNT	173.9	34.0	33

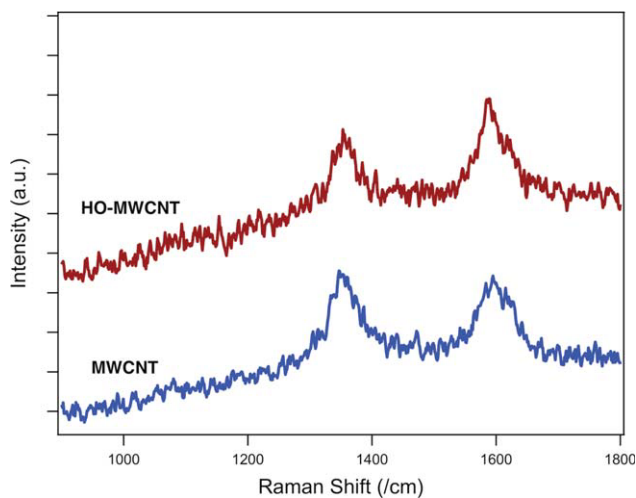


**Figure 2** Overlay of Raman spectra of 1 wt % HO-MWCNT in PVDF and 1 wt % MWCNT in PVDF. [Color figure can be viewed in the online issue, which is available at [wileyonlinelibrary.com](http://wileyonlinelibrary.com).]

from  $sp^2$  to  $sp^3$  hybridization.<sup>13</sup> In the Raman spectra collected in our samples however, the ratio of D to G band intensities appears to decrease for the sample consisting of HO-MWCNTs when compared with the sample with unfunctionalized MWCNTs. This behavior seems counterintuitive, however, it has been commonly reported for MWCNT. The explanation is that the  $sp^2$  to  $sp^3$  hybridization only occurs in the outermost nanotubes; therefore, the change in intensity of the D band relative to the G band becomes less significant. Furthermore, the D band can actually be seen to decrease in functionalized samples due to removal of defect laden amorphous carbon during the functionalization process.<sup>14,15</sup>

Solution samples consisting of 2 wt % MWCNT, a mixture of 1 wt % MWCNT and 1 wt % HO-MWCNT, and 2 wt % HO-MWCNT were prepared for scanning electron microscope (SEM) analysis. After ultrasonication, the solutions were immediately drop casted onto glass plates and placed in a pre-heated vacuum oven (70°C) for removal of the solvent. After drying, sample strips were submerged in liquid nitrogen and immediately fractured to reveal accurate cross-sectional representations. The composite films were then imaged on a cross-sectional puck at an accelerating voltage of 15 kV.

The most noticeable difference between the three samples was film thickness, namely 44  $\mu\text{m}$ , 20  $\mu\text{m}$ , and 12  $\mu\text{m}$  for the 2 wt % MWCNT sample, mix of 1 wt % MWCNT and 1 wt % HO-MWCNT, and 2 wt % HO-MWCNT, respectively. The final film thickness was repeatable for a given mixed fill concentration and is dependent on solution viscosity (on the order of 100 CP for starting PVDF solutions), which changes with fill ratio, polymer molecular weight, and concentration. As the total MWCNT weight percent of the samples was the same, the difference in thickness was attributed to the makeup and surface functionalization of the tubes, which provides an increased interaction with solvent and matrix materials leading to enhanced dispersion. Further experiments revealed that film thickness was largely dependent on weight percentage of HO-MWCNT, further verifying our assumption. Magnified images of the cross-sectional plane of the composites reveal a dense forest of tubes within the polymer. Qualitative comparison of Figures 3(B)–3(D) displays an apparent decrease in MWCNT density corresponding to direct decrease in the MWCNT content. No

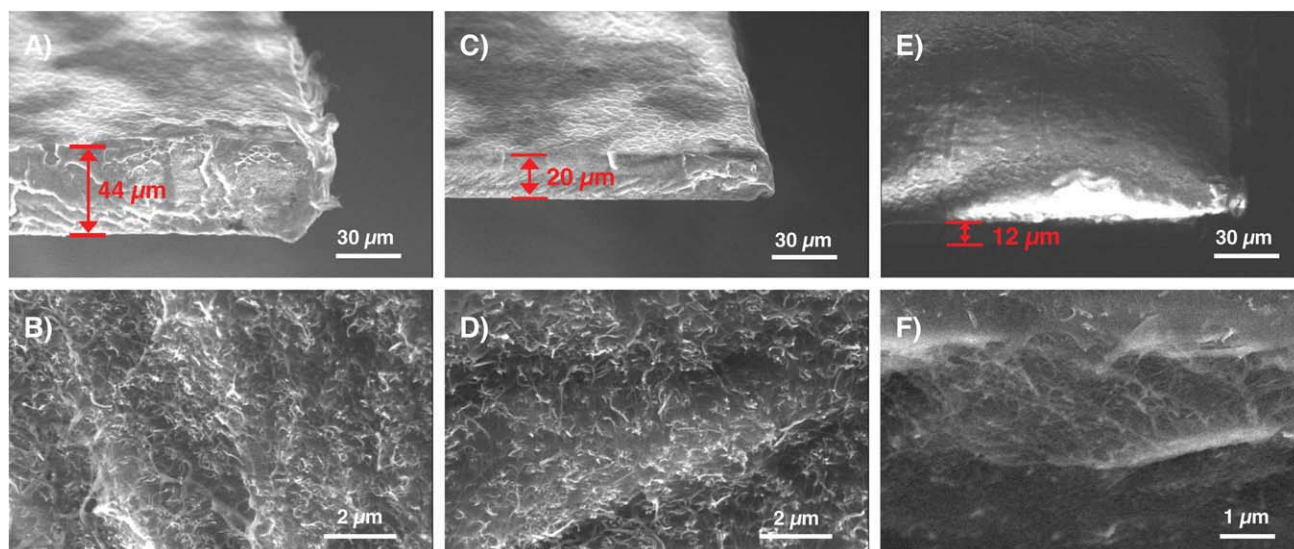


**Figure 3** Scanning electron microscope cross-sectional images of CNT-PVDF composite films with (A, B) 2 wt % MWCNT, (C, D) 1 wt % MWCNT and 1 wt % HO-MWCNT, and (E, F) 2 wt % HO-MWCNT. [Color figure can be viewed in the online issue, which is available at [wileyonlinelibrary.com](http://wileyonlinelibrary.com).]

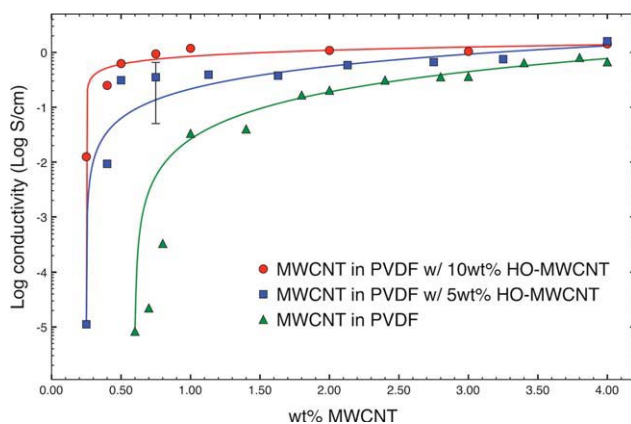


**Figure 4** Percolation plot of composites with increasing concentration of MWCNT and at three concentrations of HO-MWCNT: 10 wt % HO-MWCNT (red circle), 5 wt % HO-MWCNT (blue square), and no HO-MWCNT (green triangle). [Color figure can be viewed in the online issue, which is available at [wileyonlinelibrary.com](http://www.wileyonlinelibrary.com).]

other apparent differences between the three compositions could be detected at this level. The image quality of the 2 wt % HO-MWCNT composite is poor, relative to the other two samples, due to its insulating nature.

#### Sheet resistance of mixed fill PVDF nanocomposites

Initial studies to increase the dispersion of MWCNTs in PVDF revealed that blending mixed fill systems composed of functionalized and unfunctionalized MWCNTs resulted in a slight decrease in sheet resistance. To explore this phenomenon further, we conducted a series of electrical percolation experiments to find an optimum blend of oxidized and untreated MWCNT in PVDF. Films of nanocomposites were prepared via drop casting from solution. Circular discs of composite material with a diameter of 4 cm were cut directly on the plate and peeled off for sheet resistance measurements. The electrical conductivity of the materials, shown in Figure 4, was measured at room temperature using a four-point probe method to account for contact resistance.

Clearly, the ability of MWCNT to form an electrically conductive network is aided by the presence of oxidized MWCNT in a mixed fill system. It should be noted that PVDF composites consisting of only HO-MWCNTs exhibited strictly insulating electrical

properties; therefore, the measured conductivities of the mixed fill materials were negligibly affected by current flow through the additional HO-MWCNTs. It is possible that the dispersion of MWCNTs in a mixed fill system is much greater and aggregation of the tubes during film drying is most likely decreased. Electrical percolation in polymer nanocomposites with CNTs as the filler material has been examined extensively,<sup>16</sup> and yet improving dispersion and electron transport through nanotube contact invariably remains a challenge in homogeneous polymer nanocomposites (as apposed to segregated networks).<sup>17</sup>

The behavior of the mixed fill composites was further examined by fitting the electrical conductivity data to a power law dependence and extracting the characteristic parameters. Traditional percolation theory states that conductivity of the composites can be described by the following equation:<sup>18</sup>

$$\sigma(x) = a(x - b)^n \quad (1)$$

where  $\sigma$  is electrical conductivity,  $a$  is the saturation conductivity,  $b$  is the percolation threshold, and  $n$  is the critical exponent. The saturation conductivity of the system should theoretically approach the conductivity of the CNT. The percolation threshold is the point at which the system becomes conductive and has been found to be a function of filler aspect ratio.<sup>19</sup> The critical exponent is a function of the overall system, including fabrication of composites and resulting aggregation characteristics.<sup>18</sup> The curve fits were based on an unconstrained nonlinear minimization of the sum of squared residuals with respect to the three parameters. The extracted parameters are shown in Table II.

The percolation threshold with no oxidized MWCNTs is seen to occur at 0.49 wt % MWCNT. This threshold dramatically decreased to 0.25 wt % MWCNT when the same MWCNTs were mixed into solutions containing 5 wt % HO-MWCNT. The amount of MWCNTs needed to form a conductive network through the matrix in this case was nearly half as much. The samples had not only lower percolation but also increased overall electrical conductivity. Increasing the concentration of HO-MWCNT from 5 to 10 wt % resulted in a percolation threshold that was approximately the same as the threshold observed in 5 wt % HO-MWCNT system. However,

**TABLE II**  
Extracted Parameters for Power Law Curve Fit to Conductivity Data

Parameter	0 wt % HO-MWCNT	5 wt % HO-MWCNT	10 wt % HO-MWCNT
$a$ —Saturation conductivity	0.0187	0.1259	0.7818
$b$ —Percolation threshold	0.4916	0.2502	0.2636
$n$ —Critical exponent	3.1886	1.0186	0.9627

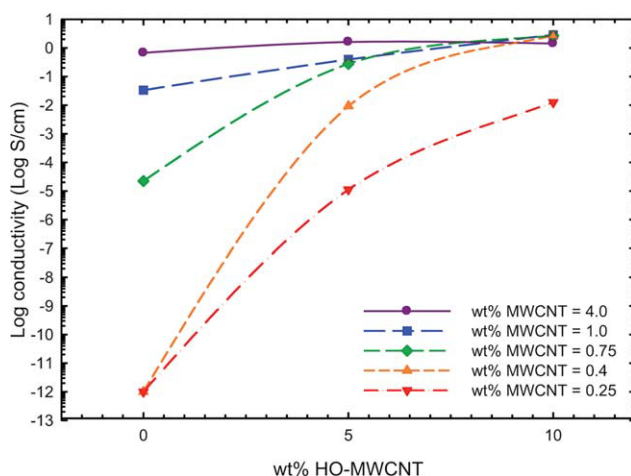


**Figure 5** Conductivity plot of composites with increasing concentration of HO-MWCNT at varying concentrations of MWCNT: 4 wt % MWCNT (purple circle), 1 wt % MWCNT (blue square), 0.75 wt % MWCNT (green square), 0.4 wt % MWCNT (orange triangle), and 0.25 wt % MWCNT (red inverted triangle). [Color figure can be viewed in the online issue, which is available at [wileyonlinelibrary.com](http://wileyonlinelibrary.com).]

comparing the lowest fractions of MWCNT (0.25 wt %), the electrical conductivity in the 10 wt % HO-MWCNT was three orders of magnitude higher than that in the 5 wt % HO-MWCNT. Finally, there was a significant change in the critical exponent with the addition of functionalized MWCNTs from around 3 to 1. As the fabrication method of all composites was the same, this observation leads to the speculation that aggregation of nanotubes was decreased in the systems with functionalized tubes.

Figure 5 illustrates the change in conductivity with increasing concentration of HO-MWCNT at varying concentrations of unfunctionalized MWCNTs. For the composites containing 0.25 and 0.4 wt % with no HO-MWCNTs, there is no measurable conductivity and is plotted at  $10^{-12}$  S  $\text{cm}^{-1}$  to reflect the limitations of the measurement device. As the amount of MWCNTs is increased, the benefits of the addition of functionalized MWCNTs decrease. At around 4.0 wt % MWCNT, the effect appears negligible. At this loading, it is likely that there is sufficient amount of MWCNTs present to make aggregation a nonissue. Furthermore, the boost in conductivity from 0 to 5 wt % HO-MWCNT is more significant than that from 5 to 10 wt % HO-MWCNT, suggesting there is some saturation limit to the benefits of incorporating HO-MWCNT.

## CONCLUSIONS

Nanocomposites with varying concentration of MWCNT in PVDF were prepared with or without HO-MWCNT as a dispersant. The dispersion characteristics were examined by FTIR, which showed a

slight increase in the  $\beta$  crystalline phase of the polymer. Dispersion was also characterized by SEM analysis, which revealed a decrease in film thickness with increasing HO-MWCNT and decreasing MWCNT content, respectively, owing to a change in solution viscosity during sample preparation. The SEM analysis of the tubes showed no distinct difference other than the apparent decrease in tube density with decreasing MWCNT content. The benefit of blending functionalized HO-MWCNT into MWCNT/PVDF composites is observed from the electrical conductivity measurements of cast composite films. A power law fit of the experimental data reveals a decrease in the percolation threshold with an increase in the saturation conductivity. The percolation threshold was decreased from 0.49 to 0.25 wt %, with an increase in conductivity at the percolation threshold with only half the concentration of MWCNT (ternary composite containing 10 wt % HO-MWCNT in PVDF) compared with the binary composite without functionalized MWCNT. The improved electrical properties point toward an improved dispersion of MWCNT at lower fill percentages leading to a faster approach to the saturation conductivity observed in this system.

## References

- Baughman, R. H.; Zakhidov, A. A.; de Heer, W. A. *Science* 2002, 297, 787.
- Bose, S.; Khare, R. A.; Moldenaers, P. *Polymer* 2010, 51, 975.
- Kamaras, K.; Itkis, M. E.; Hu, H.; Zhao, B.; Haddon, R. C. *Science* 2003, 301, 1501.
- O'Connell, M. J.; Boul, P.; Ericson, L. M.; Huffman, C.; Wang, Y.; Haroz, E. H.; Kuper, C.; Tour, J.; Ausman, K. D.; Smalley, R. E. *Chem Phys Lett* 2001, 342, 265.
- Sun, Y.; Bao, H.-D.; Guo, Z.-X.; Yu, J. *Macromol* 2009, 42, 459.
- Spitalksy, Z.; Krontiras, C. A.; Georga, S. N.; Galiotis, C. *Compos A* 2009, 40, 778.
- Jung, Y. C.; Kim, H. H.; Kim, Y. A.; Kim, J. H.; Cho, J. W.; Endo, M.; Dresselhaus, M. S. *Macromol* 2010, 43, 6106.
- Liu, J.; Rinzler, A. G.; Dai, H.; Hafner, J. H.; Bradley, R. K.; Boul, P. J.; Lu, A.; Iverson, T.; Shelimov, K.; Huffman, C. B.; Rodriguez-Macias, F.; Shon, Y.-S.; Lee, T. R.; Colbert, D. T.; Smalley, R. E. *Science* 1998, 280, 1253.
- Gregorio, R., Jr. *J Appl Polym Sci* 2006, 100, 3272.
- Zhao, X.; Cheng, J.; Chen, S.; Zhang, J.; Wang, X. *J Polym Sci Part B: Polym Phys* 2010, 48, 575.
- Pan, H.; Liu, L.; Guo, Z. X.; Dai, L.; Zhang, F.; Zhu, D.; Czerw, R.; Carroll, D. L. *Nano Lett* 2003, 3, 29.
- Almasri, A.; Ounaies, Z.; Kim, Y. S.; Grunlan, J. *Macromol Mater Eng* 2008, 293, 123.
- Bokobza, L. *Polymer* 2007, 48, 4907.
- Georgakilas, V.; Bourlino, A.; Gournis, D.; Tsoufis, T.; Trapalis, C.; Mateo-Alonso, A.; Prato, M. *J Am Chem Soc* 2008, 130, 8733.
- Dang, Z. M.; Wang, L.; Zhang, L. P. *J Nanomat* 2006, 83583, 1.
- Bauhofer, W.; Kovacs, J. Z. *Compos Sci Tech* 2009, 69, 1486.
- Kim, D.; Kim, Y.; Choi, K.; Grunlan, J. C.; Yu, C. *ACS Nano* 2010, 4, 513.
- Hu, N.; Masuda, Z.; Yan, C.; Yamamoto, G.; Fukunaga, H.; Hashida, T. *Nanotechnology* 2008, 19, 1.
- Celzard, A.; McRae, E.; Deleuze, C.; Dufort, M.; Furdin, G.; Mareche, J. F. *Phys Rev B* 1996, 53, 6209.